

## Karst Geothermal System in the Beijing-Tianjin-Hebei Plain of North China

WANG Xinwei<sup>1</sup>, MAO Xiang<sup>1</sup>, JI Lu<sup>1</sup>, LIU Huiying<sup>1</sup>, LUO Lu<sup>1</sup>, LI Kewen<sup>2,3</sup>, LI Haiquan<sup>1</sup> and HUANG Xu<sup>1</sup>

<sup>1</sup> Sinopec Star Petroleum Corporation Limited, Beijing 100083, China

<sup>2</sup> China University of Geosciences (Beijing), Beijing 100083, China

<sup>3</sup> Stanford University, CA 94305-4007, USA

wangxinwei.xxsy@sinopec.com, maoxiang.xxsy@sinopec.com

**Keywords:** Karst geothermal reservoir, Geothermal system, Resource Evaluation, Beijing-Tianjin-Hebei Plain

### ABSTRACT

The Beijing-Tianjin-Hebei Plain covers an area of about 87,000 km<sup>2</sup>. It is the main area for the development and utilization of carbonate Karst geothermal reservoirs in the central part of the Bohai Bay Basin, providing an accumulated heating area of more than 40 million m<sup>2</sup>. This paper presents a comprehensive study that covers aspects of reservoir-caprock assemblages, reservoir characteristics, water sources, migration pathways, and heat transfer modes of the Karst geothermal system in the Beijing-Tianjin-Hebei Plain. A conceptual model of medium-low temperature conductive aquifer system is established to representing the Karst geothermal system in the Beijing-Tianjin-Hebei Plain. It takes high geothermal heat flow of a large rift basin as background, atmospheric precipitations from Taihang and Yanshan mountains as recharge water sources, deep faults at basin margin and Karst unconformities as migration pathways. Geothermal water is heated up through deep circulations and accumulates within Karst reservoirs in the basement uplift zone. This geothermal system displays the following characteristics: (1) The water recharge area is close, but there are many migration pathways within the basin, and the migration distance is relatively long. Due to the large coverage of the rift basin, recharge water from both Taihang and Yanshan mountains migrates along four main groundwater runoff directions (i.e. low pressure zones in a basin, such as basement uplift zones and tectonic transformation zones), with the migration distance of more than 4km towards east into the sea, and the migration time of longer than 25 ka. (2) There are six types of reservoir-caprock assemblages. Influenced by the difference of denudation degree between Indosinian and Yanshanian, Jixian Wumishan Formation and Ordovician Karst geothermal reservoirs are mainly developed in the study area. And due to the control of differential uplift and fall of bedrock during extensional faulting period, six types of reservoir-caprock assemblages are mainly developed. (3) High-quality geothermal resources are mainly distributed along the basement uplift zone. The central uplift zone of Jizhong depression and the Cangxian uplift zone have not only favorable Karst facies, but also relatively shallow-buried Karst geothermal reservoirs. They are characterized by many Karstification stages, large accumulative effective thickness, good reservoir physical properties and high thermal storage temperature, which all together make them to be high-quality Karst geothermal zones. According to volumetric method, the total geothermal resource of the Karst geothermal system in the Beijing-Tianjin-Hebei Plain is estimated to be 53.821 billion GJ, which is equivalent to 184.155 billion tons of standard coal. According to current economic recoverable depth of geothermal drilling, annual recoverable geothermal resources of shallow Karst geothermal reservoirs within 4 km is equivalent to 222 million tons of standard coal and that can provide 7.65 billion square meters of heating space, which shows a great potential for geothermal development.

### 1. INTRODUCTION

The terminology of geothermal system was first proposed by Helgeson (1968) to discuss heat source, water source, lithology of geothermal reservoir, structure and hydrothermal dynamic characteristics of Salton Sea geothermal field in the United States. Rybach et al. (2015) emphasized the validity of geothermal system, pointed out clearly that only a system with enough geothermal enrichment to form energy resources can be called a geothermal system, and followed Muffler's (1976) classification scheme of geothermal system, that is, geothermal system can be divided into convective and conductive types according to its geological environment and heat transfer mode. On this basis, different scholars have further subdivided and named the types of geothermal systems according to the plate tectonic background, the temperature of hot water and the types of thermal storage media. However, they all emphasize that the study of geothermal systems generally includes the analysis of the four elements of thermal storage, caprock, thermal fluid channel (water source) and heat source, and the establishment of conceptual models to reflect their interaction processes (Arnorrsson, 1995; Nukman et al., 2013; Moeck, 2014). He et al. (2017) and Zhang et al. (2017) referred to the concept of "petroleum system" in the field of oil and gas research, and defined geothermal system as "a relatively independent thermal energy accumulation unit centered on heat source, including the geological elements needed for heat generation-migration-accumulation-maintenance and geological processes". Therefore, the study of a geothermal system should pay more attention to the analysis of the geological process of "heat transfer, storage, preservation and loss" on the basis of the four geological genetic factors study of "source (including heat source and water source), reservoir (accumulation), channel (path) and caprock (layer).

The area of Beijing-Tianjin-Hebei Plain is about 87,000 square kilometers. Its tectonic division belongs to the central part of Bohai Bay Basin. The secondary tectonic units include Jizhong Depression, Cangxian Uplift, and the local areas of Huanghua Depression and Linqing Depression (Figure 1). Its geothermal resources belong to a typical conductive geothermal system in low-and medium-temperature sedimentary basins, and are the main areas for the development and utilization of carbonate Karst geothermal reservoirs in China. The exploration and development of the Karst geothermal system in this area has mainly undergone three stages of centralized development.

The first stage started in Tianjin in 1971, with 10 geothermal anomalies delineated and eight geothermal fields explored, such as Wanglanzhuang and Shanlingzi. The second stage happened between 2009 and 2013 in Hebei Xiongxin, Sinopec invested on geothermal heating projects of 3.86 million square meters, accounting for more than 90% of the total heating area in Xiongxin County, and built the first smokeless city in the Beijing-Tianjin-Hebei region. Because of its shallow burial depth, excellent resource conditions (single well water production can meet the heating demand of more than 100,000 square meters without additional heat source after heat transfer), easy recharge, good economic benefits and other advantages, it is highly reproducible. The third is the development stage of geothermal urban agglomeration in recent years. In order to reduce carbon dioxide emissions, the "Xiongxin Model" has been rapidly promoted in the Beijing-Tianjin-Hebei area. By the end of 2017, at least 12 counties/cities, including Rongcheng, Gaoyang, Boye, Ninghe, Xianxian and Gucheng, had exploited and utilized carbonate Karst geothermal reservoirs (Table 1), drilled more than 800 geothermal wells, and accumulated heating area exceeded 40 million square meters.

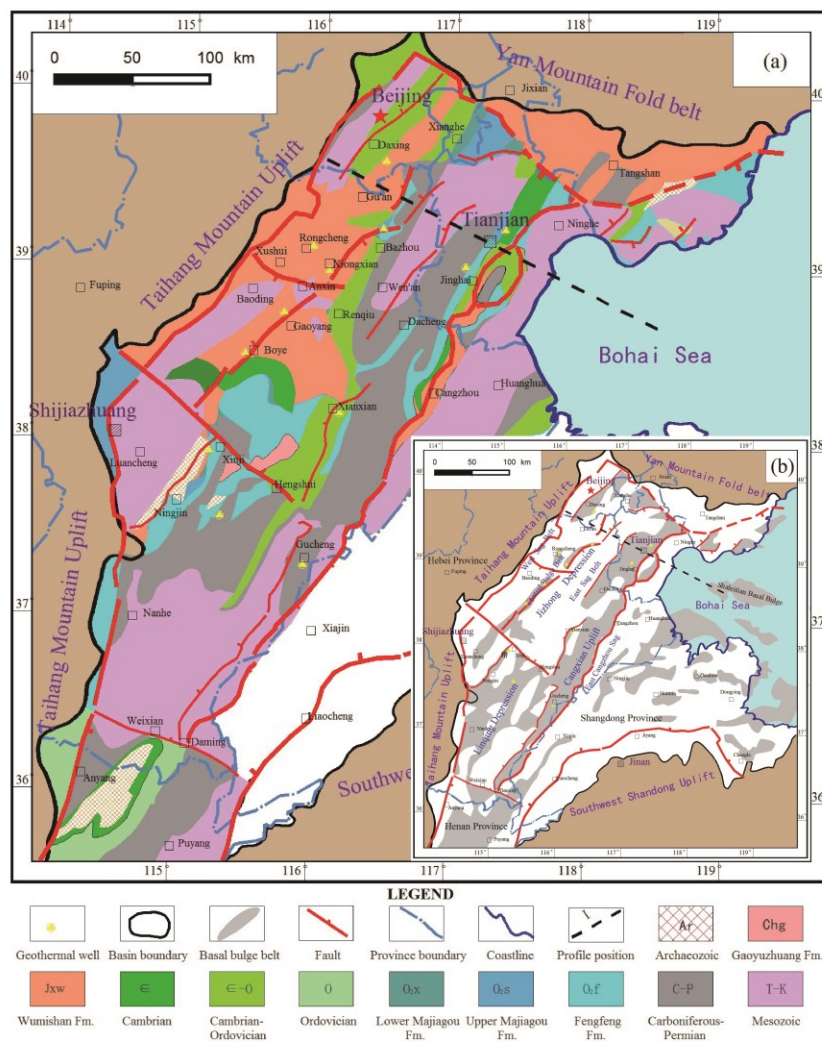


**Figure 1: Pre-Cenozoic Paleogeologic Map of the Beijing-Tianjin-Hebei Plain.**

At present, the exploration and development of carbonate Karst geothermal reservoirs are mainly concentrated in two relatively shallow buried structural belts, the central uplift belt of Jizhong Depression and the Cangxian uplift belt. The geothermal reservoirs are located in two main formations of Jixian Wumishan Formation and Ordovician System, with well depths of 1.5-4km, wellhead water temperature of 55-110°C and single well water volume of 80-120 m<sup>3</sup>/h (Table 1). Although there are more than 400 wells developing Karst geothermal reservoirs in this area, and many meaningful research work has been done in heat flow, geothermal field, heat transfer mode, geothermal resource evaluation within oil fields (Chang et al., 2016; Gong et al., 2003; Wang et al., 2002), geothermal exploration and research degree is very low for the vast Beijing-Tianjin-Hebei Plain, especially in the genetic model of Karst geothermal reservoirs in different tectonic belts, the differences of reservoir physical properties and the amount of economically exploited resources, which is far from meeting the needs of the rapid development of geothermal development and utilization. Therefore, on the basis of summarizing the previous geothermal and petroleum exploration results (Yan and Yu, 2000; Wu and Wang, 2010; Yang, 2009), and combining the latest geothermal drilling data and hydrochemical analysis data, this paper aims to compare the differences of reservoir-cap assemblage and Karstification intensity of Karst geothermal reservoirs in different structural units of the basin, analyze the spatial distribution rules of reservoir physical properties, establish the conceptual model of the formation of Karst geothermal reservoir based on the analysis of the geothermal water

transport path, and evaluate the geothermal resources of the Karst geothermal reservoirs. Altogether, it will provide technical support for large-scale development of Karst geothermal reservoirs.

**Table 1: Data statistics of Karst geothermal wells in the Beijing-Tianjin-Hebei Plain.**

Well	Location	2 <sup>nd</sup> -order Tectonic Unit	3 <sup>rd</sup> -order Tectonic Unit	Reservoir	Production Interval /m	Wellhead temperature /°C	Production Rate /m <sup>3</sup> /h
XR9	Daxing	Northern part of Central Bulge	South slope of Daxing Bulge	Jxw	3,200-3,620	117	92
BR5	Bazhou	Northern part of Central Bulge	Northern part of Niutuozen Bulge	Jxw	2,980-3,342	104	140
BZC2	Xiongxian	Northern part of Central Bulge	Southern part of Niutuozen Bulge	Jxw	850-1,500	68	115
CN1	Rongcheng	Northern part of Central Bulge	Rongcheng Bulge	Jxw+Chg	850-1,900	55	110
XF1	Gaoyang	Central part of Central Bulge	Northern part of Gaoyang low Bulge	Jxw	3,200-3,500	106	50 (natural flowing)
DF1	Boye	Central part of Central Bulge	Southern part of Gaoyang low Bulge	Jxw	3,165-3,758.17	110	97
GJC2	Xinji	Southern part of Central Bulge	Ningjin Bulge	O+∈	2,460.6-2,622	86	86.8
XH10	Xinhe	Southern part of Central Bulge	Xinhe Bulge	O	1,205.6-1,502.1	62	112.78
ZJC1	Ninghe	Northern part of Cangxian Uplift	Panzhuang Bulge	Jxw	2,384-3,080	85	112
GD1	Tianjin	Northern part of Cangxian Uplift	Shuangyao Bulge	O	1,900-2,300	65	115
XD3	Xianxian	Central part of Cangxian Uplift	Xianxian Bulge	Jxw	1,382.5-1,698	96	150
XY1	Gucheng	Southern part of Cangxian Uplift	Wucheng Bulge	O+∈	2,095.48-3,000	85	69

## 2. EVOLUTION STAGES OF THE KARST GEOTHERMAL SYSTEM

The Bohai Bay Basin is a large Cenozoic rift basin, which is characterized by a wedge-shaped deposit controlled by extensional faults in the Paleogene and an overall depression deposit in the Neogene. The regional stratigraphic-tectonic framework (Figure 2) reveals that only the Cenozoic stratigraphic thickness in the deepest depression of the Beijing-Tianjin-Hebei Plain is more than 8km (Dong et al., 2013; Zhang et al., 2001). The evolution of the basin basement mainly experienced two stages: the shallow-sea platform deposition from middle-late Proterozoic to Paleozoic, and the compression and folding movements from Mesozoic Indosinian to Yanshanian. The maximum stratigraphic thickness is more than 7km (Qiao et al., 2002). According to the influence of regional tectonic-sedimentary evolution on the genesis of Karst geothermal system, the formation process of Karst geothermal system in the Beijing-Tianjin-Hebei Plain is divided into the following five stages (Figure 3):

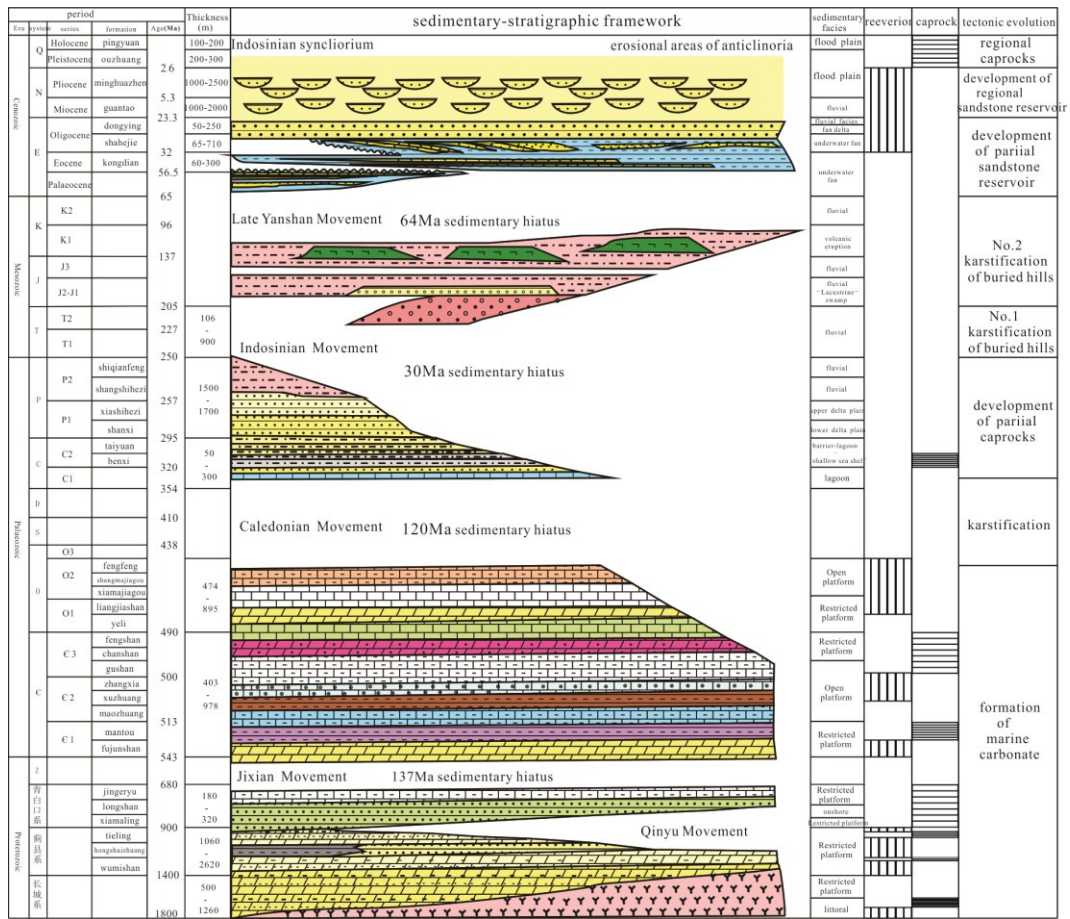


Figure 2: Sedimentary and stratigraphic framework of the Beijing-Tianjin-Hebei Plain.

(1) The middle Proterozoic-Early Paleozoic platform-type marine carbonate deposition stage. Tectonic movements during this period were dominated by overall lifting and falling. Sedimentation developed thick marine carbonates of the Middle-Late Proterozoic Changcheng-Jixian System and the Early Paleozoic Cambrian-Ordovician, with an overall thickness of more than 5km, which constituted the material basis for the formation of Karst geothermal reservoirs (Figure 3a). Among them, the middle-late Proterozoic deposits were dominated by the dolomites of the Wumishan Formation in the Jixian System, with a thickness of 2-3km. The Lower Paleozoic was dominated by Ordovician limestones with a thickness of 600-800m. During this period, the overall crustal uplifting movement occurred at least three times, including the Qinyu Movement, the Jixian Movement and the Caledonian Movement, and it was characterized by the regional uplift at the end of the Caledonian period. The resulting cessation of deposition and relatively flat Karst paleo-geomorphology led to the formation of Karst caves and pores along layers.

(2) The late Paleozoic overlying caprock development stage. The overall subsidence of the North China Plate during the Late Paleozoic resulted in the deposition of the marine-continental coal-phase stratum with a thickness of about 800-1,200m in the Beijing-Tianjin-Hebei Plain, forming the overlying caprock of the Ordovician marine carbonate Karst geothermal reservoir (Figure 3b).

(3) The Mesozoic uplift and subsequent erosion and buried hill type Karst development stage. The Mesozoic Indosinian and Yanshanian tectonic movements resulted in strong compression and uplift of regional strata, and formed the modern NE-oriented tectonic framework. The denudation caused by tectonic deformation was strong in the west and weak in the east, that is, the western tectonic belt formed the ancient western Hebei anticlinorium, and the exposed stratum is the Wumishan Formation of the Jixian System, while the eastern tectonic belt formed the ancient Cangzhou-Tianjin Syclnorium, and the exposed stratum is the upper part of the Ordovician (Figure 3c). At the same time, the paleo-geomorphic height difference of more than 2km formed by folding revealed characteristics of buried hill type Karstification, that is, lateral zoning and vertical stratification. Laterally, it could be divided into three Karst facies belts, including Karst highland (the ancient Western Hebei Anticlinorium), Karst slope (the Central Hebei Slope), and Karst depression (Cangzhou-Tianjin Syclnorium). Vertically, it could be divided into three intervals, including vertical vadose zone, horizontal underflow zone and deep corrosion zone.

(4) The stage of differential uplift-subsidence of the Paleogene extensional fault blocks and the development of fault-related Karstification. The deposition in this period was characterized by the rifted deposition under the control of large extensional faults (Figure 3d). The footwall rose and eroded, and the buried hill-type Karstification was further enhanced. With the continuously enhanced extension and deposition, the hanging wall developed hydrothermal corrosion associated with Karstification and organic acid corrosion associated with source rock maturation along the fault plane. At the same time, due to the influence of the differential development of the extensional

fault blocks, the ancient Western Hebei-anticlinorium and the ancient Cangzhou-Tianjin Synclinorium changed, correspondingly, the structural elevation also underwent major changes, that is, the ancient Western Hebei Anticlinorium evolved into Central Hebei Depression, and the ancient Cangzhou-Tianjin Synclinorium evolved into the Cangxian Uplift.

(5) The formation stage of Neogene geothermal reservoir caprock and Karst aquifer systems. In Neogene, the crust overall sank, deposited fluvial clastic sediments with a thickness of 1.7-2km, which formed the regional cap rock for Karst geothermal reservoirs. At the same time, the Taihang Mountain on the west side rose speedily, providing the Karst geothermal reservoirs in the basin with the recharge water source and the power of deep recirculation of geothermal water. Under the background of the high geothermal flow value of the extension basin, a vast aquifer system of Karst geothermal reservoirs was formed under the Beijing-Tianjin-Hebei Plain.

It can be inferred from the above that there are mainly four stages and three types of Karstification that determine the performance of Karst geothermal reservoirs, namely, the interlayer Karstification during the Caledonian overall uplift, the buried hill-type Karstification during the Indosinian and the Yanshanian squeezing and subsequent uplifting movements, and the burial Karstification associated with the Himalayan extensional faults.

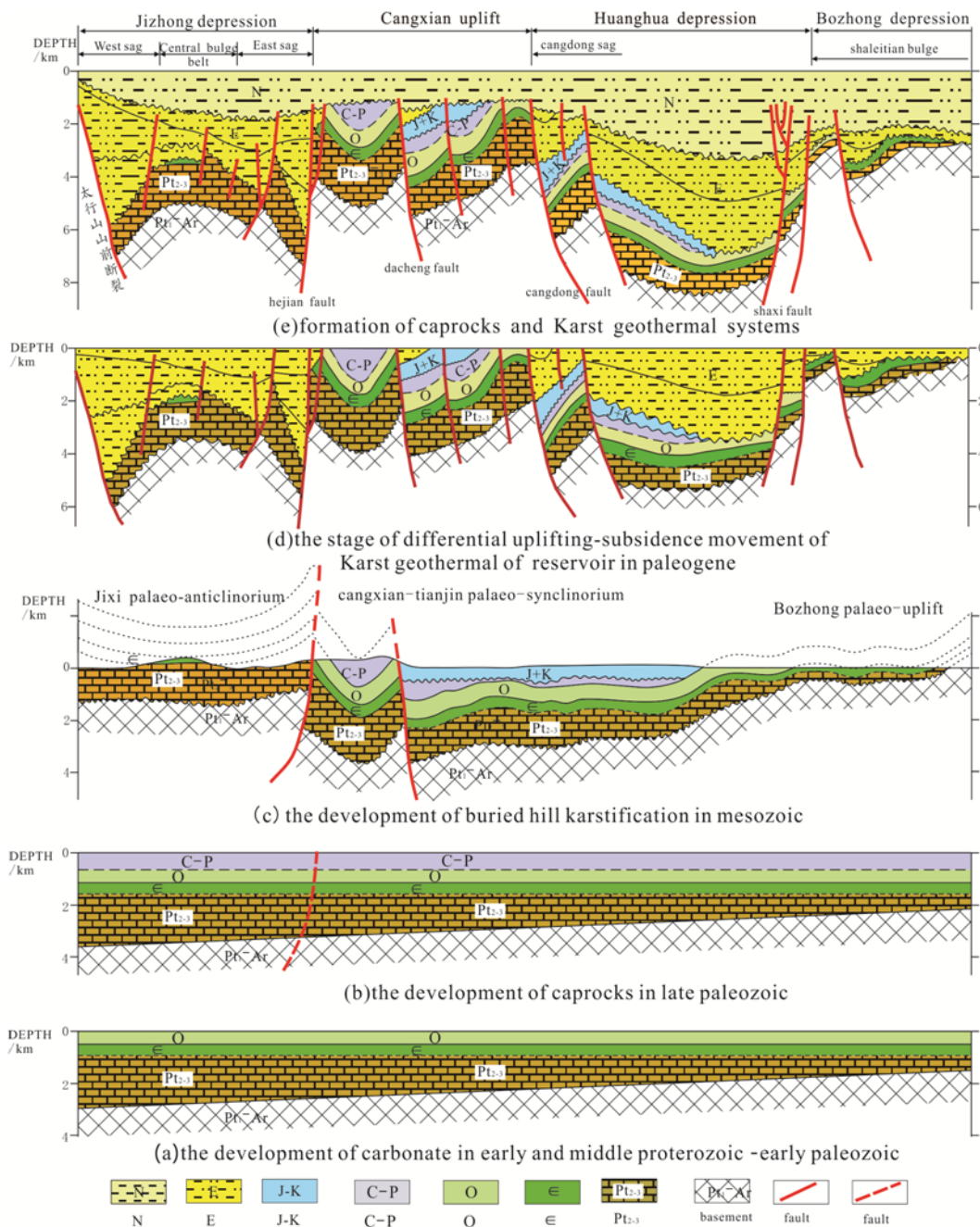


Figure 3: Evolution stages of Karst geothermal reservoirs in the Beijing-Tianjin-Hebei Plain.

### 3. GENESIS OF KARST GEOTHERMAL SYSTEM

#### 3.1 Reservoir-caprock assemblages

The overlying caprock of the Karst geothermal reservoirs in the study area was the Carboniferous-Permian coal-bearing strata, and the regional caprock was the Neogene thick siliciclastic rock. They both had good sealing effects to heat. Due to the great difference in the degree of denudation caused by the Indosinian and Yanshanian movements, there were significant differences in both residual situation of the bedrock strata and the development state of the caprock among different tectonic zones. The phenomenon reflected on the different reservoir-caprock combination of Karst geothermal reservoirs in different tectonic zones. In this paper, six types of reservoir-caprock assemblages are classified according to the difference between Karst geothermal reservoirs and their overlying caprock (Figure 4).

(1) The Neogene/the Jixian System Wumishan Formation type (N/Jxw) is mainly distributed in the central bulge of the Central Hebei Depression and the local basal bulges of the Cangxian Uplift (such as the Xianxian bulge). The contact relationships between geothermal reservoirs and their overlying caprock showed that the Jixian System Wumishan Formation was directly covered by the Neogene regional caprock. The upper strata of the Paleogene and the Jixian System, developed between the geothermal reservoirs and their overlying caprock were denuded. It was characterized by the longest sedimentary discontinuity between the caprock and the reservoir, and the Karst reservoir experienced the multi-stage Karstification including the Indosinian, the Yanshanian and early Himalayan Karstifications. Karst geothermal reservoirs located in these zones usually have good reservoir properties and shallow burial depth, and therefore are preferred targets for geothermal exploration and development (Figure 4a).

(2) The Mesozoic-Cenozoic/Jixian System Wumishan Formation type ((Mz+Rz)/Jxw) is mainly distributed in the western sag and the eastern sag of the Central Hebei Depression, and the tectonic setting was the strong Indosinian-Yanshanian denudation and the superimposed extensional fault depression developed in Yanshanian or (and) early Himalayan. This type of geothermal reservoirs is characterized by good reservoir properties but deep burial depth (4-6km), which is the exploration target for deep high-temperature geothermal reservoirs (Figure 4b).

(3) The Cenozoic/the Cambrian type (Rz/Є) is mainly distributed in the Hengshui structural belt of the Central Hebei Depression and the Shuangyao bulge of the Cangxian Uplift. The tectonic setting was the strong Indosinian-Yanshanian denudation, the upper strata of Permian-Cambrian were denuded, and the Cenozoic rifted deposits were covered. The type is characterized by good reservoir properties, and shallow burial depth (1.5-2km), therefore, the zone where this type developed is a favorable exploration target for the Cambrian Karst geothermal reservoir (Figure 4c).

(4) The Cenozoic/the Ordovician type (Rz/O) is mainly distributed in the zones with shallow burial depth, such as Ningjin Bulge of the central bulge in the Central Hebei Depression and Xinhe Bulge and Guantao Bulge in the Linqing Depression. The strata experienced relatively strong Indosinian-Yanshanian denudation, the Permian-Carboniferous caprock was eroded completely, and the Ordovician Karst geothermal reservoir was covered by the Cenozoic regional caprock. A great contact relationship of reservoir and caprock formed. The type is characterized by good reservoir properties of the Ordovician reservoir and the shallow burial depth (1-1.5km), which is another regional exploration and development target (Figure 4d).

(5) The Mesozoic-Cenozoic/the Ordovician type ((Mz+Rz)/O) is mainly distributed in the structural belts with relatively deep burial depth, such as the Wuqing sag on the north side of the eastern sag in the Central Hebei Depression, and the Nangong sag of the Linqing Depression. The Indosinian-Yanshanian denudation of this type was the same as that of the Rz/O type and the Permian-Carboniferous caprock was also eroded completely. The difference is that the Ordovician reservoir of the (Mz+Rz)/O type is covered by the Mesozoic, and the rifted sediments of the Cenozoic are relatively thick. The type is characterized by good reservoir properties of the Ordovician reservoir, however, the burial depth of the reservoir was deep (4-6km), the zone where this type developed is a high-risk area for Ordovician Karst geothermal reservoir exploration (Figure 4e).

(6) The Upper Paleozoic-Cenozoic/Ordovician type ((Pz<sub>2</sub>+Mz+Rz)/O) is mainly distributed on both sides of the Cangxian Uplift and the slope transition zone between the sag and bulge in the Linqing Depression. It shows that the Permian-Carboniferous caprock overlying the Ordovician Karst geothermal reservoir and the regional Cenozoic caprock are both well developed. The strata experienced relatively weak Indosinian-Yanshanian denudation, and only the top part of the Permian-Carboniferous caprock were denuded. In the Cenozoic period, with the influence of the rotation and skew of the extensional fault blocks, there was an obviously angular unconformity contact relationship between the Permian-Carboniferous caprock and the Cenozoic regional caprock. The (Pz<sub>2</sub>+Mz+Rz)/O type had two characteristics, one was that the Ordovician Karst geothermal reservoir experienced less exposure time, and less Karstifications, therefore, the reservoir had strong heterogeneity; the other one was that the high-quality reservoir was mainly controlled by faults. The basal bulge controlled by the extensional fault was a favorable zone for Karst geothermal reservoir exploration (Figure 4f).

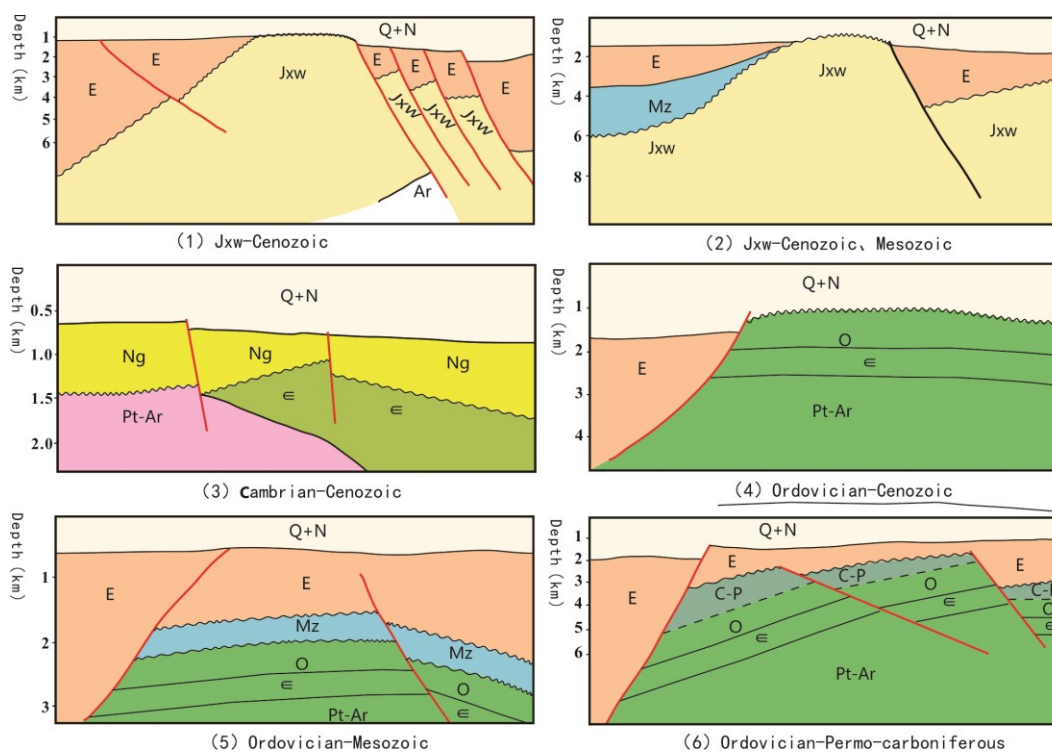


Figure 4: Six types of reservoir-caprock assemblages in the Beijing-Tianjin-Hebei Plain.

### 3.2 Reservoir characteristics

The carbonate geothermal reservoirs in the Beijing-Tianjin-Hebei Plain are of Middle-Upper Paleozoic-Lower Paleozoic. The basal geological map (Figure 1) and the tectonic-stratigraphic framework map (Figure 2) revealed that the Middle-Upper Proterozoic geothermal reservoirs were mainly the dolomites of the Jixian System Wumishan Formation, distributed in the central and northern part of the Central Hebei Depression and the northern part of the Jixian Uplift with strong regional deformations and high degree of denudation. The Lower Paleozoic geothermal reservoirs are mainly Ordovician limestones and are distributed in the zones where the denudation was weak, such as the Jixian Uplift and the Linqing Depression. The favorable Karst facies such as Karst highlands and Karst slopes, formed by the Caledonian, Indosinian and Yanshanian uplifting movements, and the favorable sedimentary facies such as reef flats, algae flats and tidal flats determined good geothermal reservoir properties.

According to the geothermal drilling data and oil drilling data in the Beijing-Tianjin-Hebei Plain, acoustic time, resistivity and gamma well log data of the Middle-Upper Proterozoic and Lower Paleozoic carbonates were used to calculate the porosity and permeability of the geothermal reservoir. The carbonates with porosity greater than 1.8% and permeability greater than 0.1mD were classified as the geothermal reservoirs. Based on this classification standard, reservoirs were classified and evaluated. The reservoir thickness map, the porosity map and the temperature map of the geothermal reservoir surface were made to illustrate the relationships between the distribution of Karst geothermal reservoirs and basin structure characteristics.

#### 3.2.1 Effective thickness

The effective thickness of Karst geothermal reservoirs in the Beijing-Tianjin-Hebei Plain is referred to the cumulative thickness of reservoir intervals which were classified by the logging curves, and its distribution was mainly controlled by paleo-geomorphic highlands formed by the Indosinian and Yanshanian Karstifications. The depth of the vertical vadose belt and the horizontal undercurrent belt developed on the top part of the Karst highlands and Karst slopes of the Karst paleo-morphology determines the effective reservoir thickness. The average thickness map of buried hill-type reservoirs in the Beijing-Tianjin-Hebei Plain (Figure 5) showed that the Karst geothermal reservoirs of the Jixian System Wumishan Formation are mainly distributed in the central and northern parts of the Central Hebei Depression and the northern parts of the Cangxian Uplift. With the influence of the Indosinian, Yanshanian and Himalayan Karstifications, the effective thickness varies greatly, and the distribution characteristics are consistent with the main tectonic direction (NNE). In the eastern parts of the Central Hebei Depression with strong deformation, the effective thickness is 600-700m, and it is reduced to 300-500m in the central and western parts of the depression. Similarly, the effective thickness of the eastern edge of the Cangxian Uplift reaches 600-700m, and gradually decreases to 300m in the northeastern part.

The Ordovician Karst geothermal reservoirs are mainly distributed in the southern parts of the Cangxian Uplift and the Linqing Depression. The cumulative effective thickness of the Ordovician reservoir is smaller than that of the Jixian System Wumishan Formation, ranging from 100 to 150 m, which is related to the Caledonian Karstification formed by the overall uplift. In the structural belts with strong deformation during the Indosinian and Yanshanian periods, the effective thickness of Karst geothermal reservoirs is slightly larger.

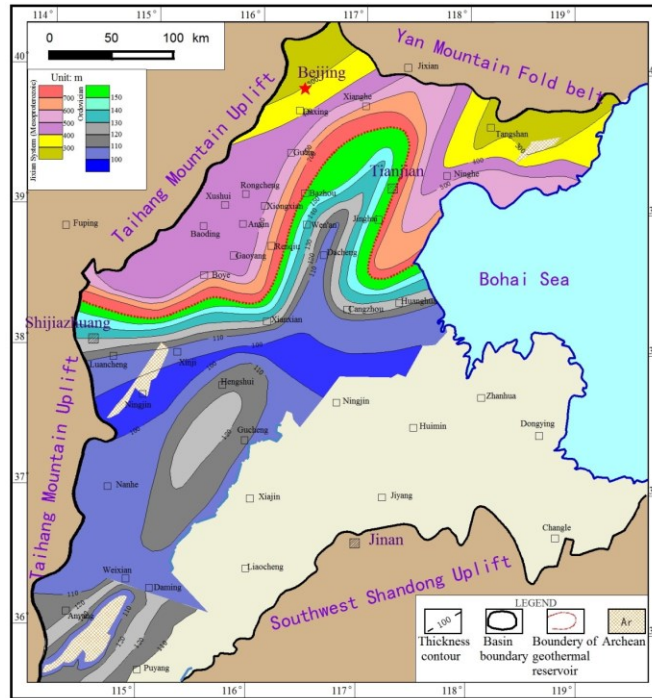


Figure 5: Average thickness map of the buried hill type geothermal reservoirs in the Beijing-Tianjin-Hebei Plain.

### 3.2.2 Porosity distribution

The porosity discussed here refers to the weighted average porosity of each type of reservoirs interpreted by the log curves. The average porosity map of Karst geothermal reservoirs in the Beijing-Tianjin-Hebei Plain (Figure 6) reveals that the distribution of the average porosity of Karst heat storage is significantly controlled by the NE-oriented structure and the Karst paleo-geomorphology. In the central bulge of the Central Hebei Depression and the Cangxian Uplift, the porosity is relatively high, ranging from 5% to 7%. In the western sag of the Central Hebei Depression and the Linqing Depression, the porosity is low, ranging from 3% to 5%. It can be inferred that the central bulge of the Central Hebei Depression and the Cangxian Uplift are targets with better reservoir properties.

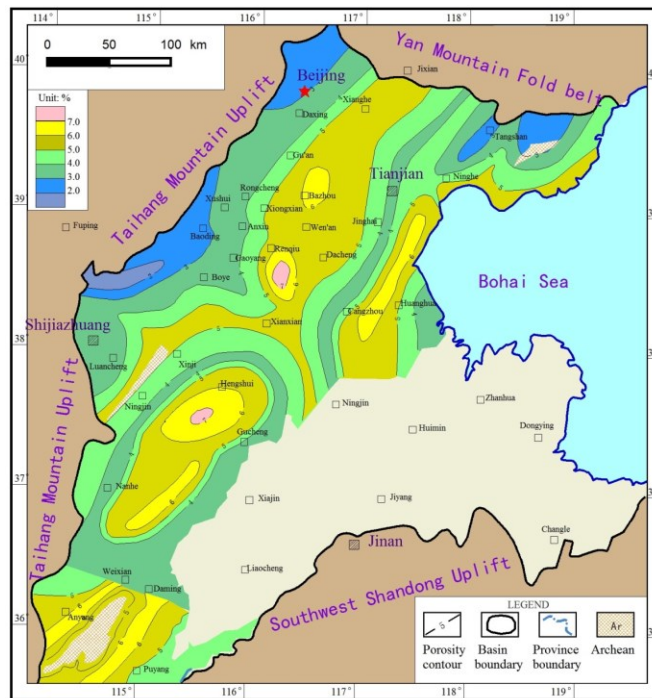


Figure 6: Average porosity map of Karst geothermal reservoirs in the Beijing-Tianjin-Hebei Plain.

### 3.2.3 Roof temperature of geothermal reservoirs

The roof temperature of geothermal reservoirs in the Beijing-Tianjin-Hebei plain is mainly controlled by the buried depth of the top of the geothermal reservoir. The lateral temperature distribution is consistent with the NE-oriented basal structural framework, with low values in basal bulge zones but high values in basal depression zones. In addition, due to the cold water injection into the recharge area of the geothermal water, the geothermal reservoir temperature in the depression at the edge of the basin is the lowest. The specific performance is as follows: in the central bulge of the Central Hebei Depression and the Cangxian Uplift, the buried depth of the geothermal reservoir is about 1.5-2.5km, and the temperature of the Karst geothermal reservoir is about 70-100 °C. In the eastern sag of the Central Hebei Depression (ie Wuqing Sag - Baxian Sag - Raoyang Sag - Shulu Sag), the Cangdong Sag, and the Nangong Sag and the Qiuxian Sag of the Linqing Depression, because the buried depth of the geothermal reservoir is deeper than 4km, the temperature of the top of the geothermal reservoir is above 100-120 °C. In the western sag of the Central Hebei Depression and the northern edge of the basin, the temperature of the top of the geothermal reservoir is less than 50-60 °C due to the cold water injection from the Taihang Mountain and Yanshan Hills, which are the geothermal water recharge areas.

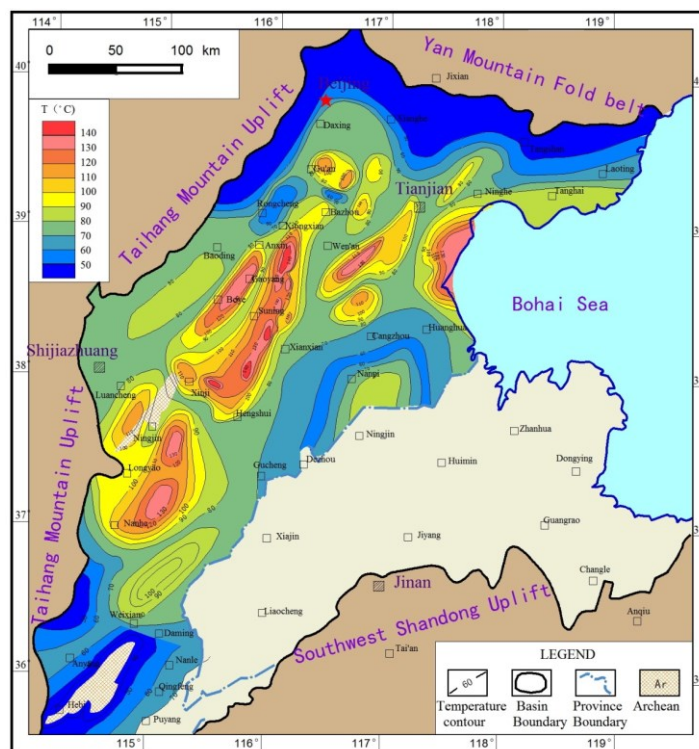


Figure 7: Roof temperature contour map of Karst geothermal reservoirs in the Beijing-Tianjin-Hebei Plain.

### 3.3 The migration path of geothermal water

The North China Plain is not only a huge surface catchment basin, but also a catchment basin for deep groundwater. Since the basement of the basin has formed a series of special structural conditions that was bumpy disparity in Meso-Cenozoic, the hydrogeological characteristics and hydrodynamic conditions of each structural part are different, which makes the runoff condition and direction of the basement groundwater in the basin have significant differences between different structural parts and depths (Zhou, 1987). In order to systematically study the geothermal water migration path of the Karst geothermal system in the Beijing-Tianjin-Hebei Plain, hydrogen and oxygen isotope analysis, hydrochemical analysis and  $^{14}\text{C}$  dating analysis were performed on 369 Karst geothermal water samples from 58 wells in different tectonic belts, of which the purpose is to analyze the source, flow direction and residence time of Karst geothermal water.

#### 3.3.1 Hydrogen and oxygen isotope analysis

From the  $\delta\text{D}-\delta^{18}\text{O}$  correlation figure (Figure 8) of geothermal water in the Karst system of the Beijing-Tianjin-Hebei Plain, it can be seen that the values of  $\delta\text{D}$  and  $\delta^{18}\text{O}$  in geothermal water are between  $-90.4\text{‰}$ ~ $-57.36\text{‰}$  and  $-12.45\text{‰}$ ~ $-6.99\text{‰}$ , respectively, as well as the average values are  $-75.72\text{‰}$  and  $-9.99\text{‰}$ , respectively. The linear relationship between  $\delta\text{D}$  and  $\delta^{18}\text{O}$  of most geothermal water samples is basically consistent with the atmospheric precipitation line in North China, indicating that the geothermal water of the Karst system in the Beijing-Tianjin-Hebei Plain comes from atmospheric precipitation. The geothermal water sample located on the right side of the atmospheric precipitation line reflects the phenomenon of oxygen shift caused by the reaction of geothermal water with the surrounding rock during the migration process.

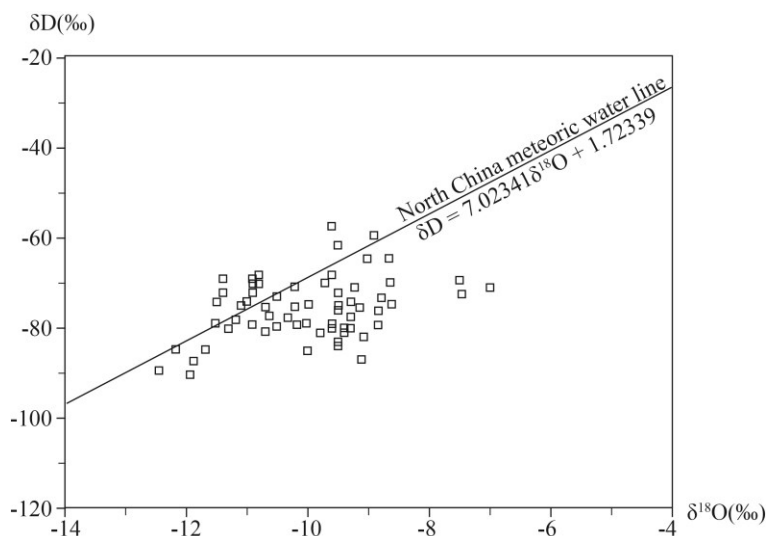


**Figure 8: The  $\delta D$ - $\delta^{18}O$  correlation diagram of geothermal water in the Karst system of the Beijing-Tianjin-Hebei Plain.**

### 3.3.2 Geothermal water chemistry characteristic

The caves and fissures in the carbonate rocks of the Middle-Upper Proterozoic-Early Paleozoic in the Beijing-Tianjin-Hebei Plain are well-developed and have good connectivity, which is in the depth of 500m below the bedrock surface and could form a good regional groundwater migration channel. The groundwater in the deep layer of the basin is confined water. After replenishment, the groundwater in the horizontal and vertical direction is mainly driven by the potential energy formed by the difference of water level and pressure, obeying the law of fluid motion and always flowing from the high water level to the low water level, and from the high pressure zone to the low pressure zone (Zhou, 1987). The variation of geothermal ion content and salinity in different tectonic zones can reflect the difference in geothermal water flow process and flow direction. In this paper, based on the previous data and sample analysis results to summarize the geothermal water hydrochemistry type and salinity distribution characteristics in the study area (Figure 9), the following points can be obtained:

(1) The distribution characteristics of the salinity value are that the marginal recharge zone is lowest (<0.4g/L), the bedrock bulge zone is lower (<3g/L), and the bedrock sag zone is higher (9-50g/L). Among them, the maximum salinity of the western sag belt and eastern sag belt in the Jizhong depression, Huanghua depression and Jiyang depression are 9g/L, 12g/L, 15g/L and 50g/L, respectively. It is reflected that the water source comes from the Taihang Mountains and the Yanshan Mountains, and transports through the pre-mountain faults and unconformity migration channels. The geothermal water shows the change law from fresh water to low mineralized water to high mineralized water to brine. The value of salinity is positively correlated with the length of the fluid migration distance.

(2) According to the principle of the sparse direction of the Karst geothermal water mineralization contour is the mainstream direction of deep groundwater runoff, it can be identified that there are mainly four groundwater runoff paths in the Beijing-Tianjin-Hebei Plain Area. Among them, the groundwater from the Yanshan Mountains in the north and the northern part of the Taihang Mountains are divided into two branches, one is moving the south along Daxing bulge, the Rongcheng bulge, and the Niutuozen bulge in the central bulge belt of the Jizhong Depression; the other is moving the south along the Panzhuang bulge, the Shuangyao bulge, and the Dacheng bulge in the Cangxian uplift belt. The groundwater from the western Taihang Mountain area are also divided into two branches. One is that the central groundwater is injected along the Xushui-Anxin lateral tectonic transition belt, and passes through the Gaoyang low bulge to the south and disappears into the sags on both sides. The other is the southern groundwater flows from the Guangzong bulge and the Minghuazhen bulge to the Gucheng bulge. After converging with the southward runoff of the Jixian uplift, it migrates eastward along the Suining uplift and enters the Bohai Bay.

(3) On the path of migration, the hydrochemistry types in the piedmont sag zone are  $HCO_3^-$ - $Ca^{2+}$ ,  $HCO_3^-$ - $Ca^{2+}$ • $Mg^{2+}$ . The hydrochemistry types in the central bulge belt of the Jizhong depression and the Cangxian uplift are  $Cl^-$ • $HCO_3^-$  - $K^+$ • $Na^+$ ,  $Cl^-$ • $SO_4^{2-}$ - $Na^+$ , respectively. The hydrochemistry types in the eastern sag belt of the Jizhong depression and the Linqing depression are  $Cl^-$ - $Na^+$ . The evolution characteristics of hydrochemistry types varies from simple to complex to simple, reflecting the variation discipline of groundwater recharge-cycle alternation-slipping-storage.

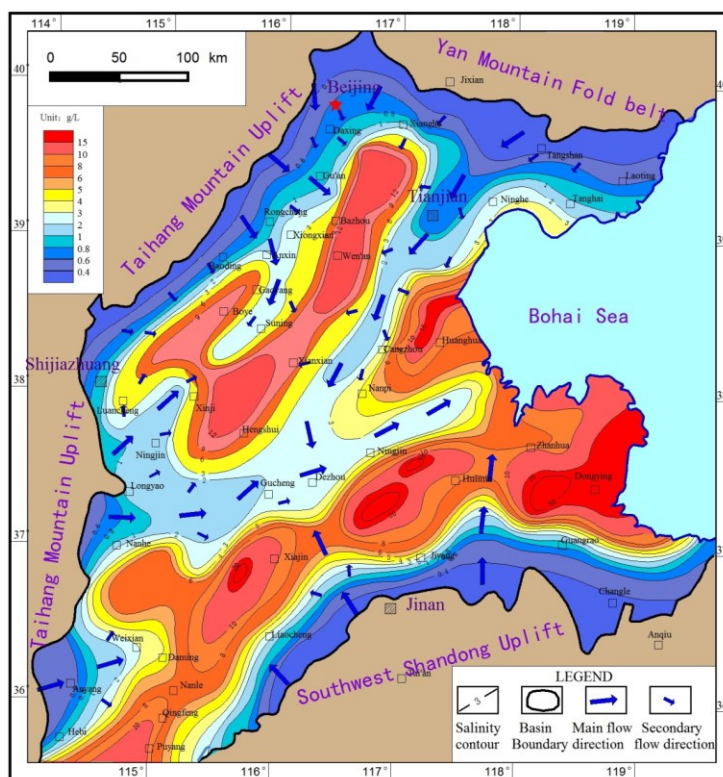


Figure 9: The geothermal water mineralization contour of the Karst geothermal system in the Beijing- Tianjin- Hebei Plain.

3.3.3 <sup>14</sup>C dating analysis

The <sup>14</sup>C isotope age of geothermal water reflects the "residence" time of the tritium free water in the geothermal reservoir, that is the time from infiltration to the recharge area, through deep circulation, runoff in the geothermal reservoir to discharge. Zhou (1987) measured the <sup>14</sup>C isotopic age of HCO<sup>3-</sup>-Na<sup>+</sup> water in the Karst geothermal reservoir of the southern wing of Daxing bulge to be 17010±270a. In this paper, based on the results of previous tests (Chen et al., 1998; Zhang et al., 2000), the <sup>14</sup>C age contour diagram of Karst geothermal water in the northern part of the Beijing-Tianjin-Hebei Plain Area was compiled (Figure 10). The figure clearly reveals the characteristics that the <sup>14</sup>C isotope age of the geothermal water gradually increases from the recharge area to the runoff area to the residence area. The specific performance is as follows: the age of the basin edge recharge area is the smallest, less than 10ka; the age of the geothermal runoff area such as the Cangxian uplift belt and the Xushui-Anxin lateral tectonic transition belt in the basin is smaller, between 10 and 15ka; In the Jizhong depression, Huanghua depression and other geothermal water residence areas, the age becomes larger, about 15 - 25ka; the highest value appears in the Bazhou sag of the Jizhong depression and the Banqiao sag of the Huanghua depression, larger than 25ka, such as the <sup>14</sup>C corrected age of the Xiong 3 well in Xiongxian is 33.536 ka (Chen et al., 1998).

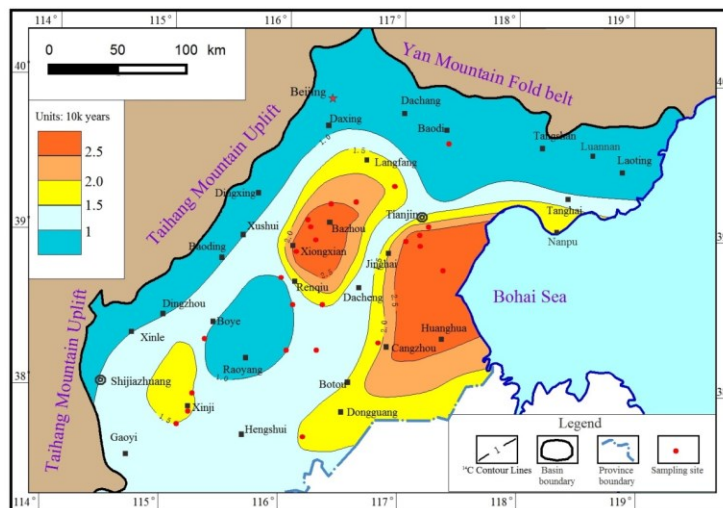


Figure 10: The <sup>14</sup>C age contour diagram of Karst geothermal water in the northern part of the Beijing-Tianjin-Hebei Plain Area (modified after Chen et al., 1998).

### 3.4 The heat transfer pattern

The heat source of the Karst geothermal system in the Beijing-Tianjin-Hebei Plain comes from the high geothermal flow value of the rift basin. The heat transfer pattern is mainly heat conduction, and there is no additional heat source such as magmatism (Mao, 2018). Many scholars have discussed the differential aggregation feature of the geothermal heat flow on the plane in the study area, that is, the heat flow value of the bedrock bulge is high (64-92 mW/m<sup>2</sup>), and the heat flow value of the bedrock sag is low (50-58 mW/m<sup>2</sup>) (Chang et al., 2016; Gong et al., 2003). At the same time, on the bedrock bulge belt, the geothermal flow value also has a large difference due to the difference in the amplitude of the bulge. For example, the heat flow value of the southern high bulge area in Niutuozen bulge (Xiong County) is as high as 92mW/m<sup>2</sup> and the heat flow value of Ningjin sag is about 75mW/m<sup>2</sup>. The heat flow value of Wucheng bulge in the middle section of Cangxian Uplift is about 80mW/m<sup>2</sup>. The heat flow value of Qinghe bulge in Linqing depression is about 65mW/m<sup>2</sup>. The difference in geothermal flow values is the result of the interaction of geothermal gradients and thermal conductivity in different tectonic zones. In this paper, four typical drilling temperature-depth curves (Figure 11) were selected as the basis to analyze the difference in the geothermal gradient between the reservoir and the caprock in different bulge belts and the thermal conductivity (Table 2).

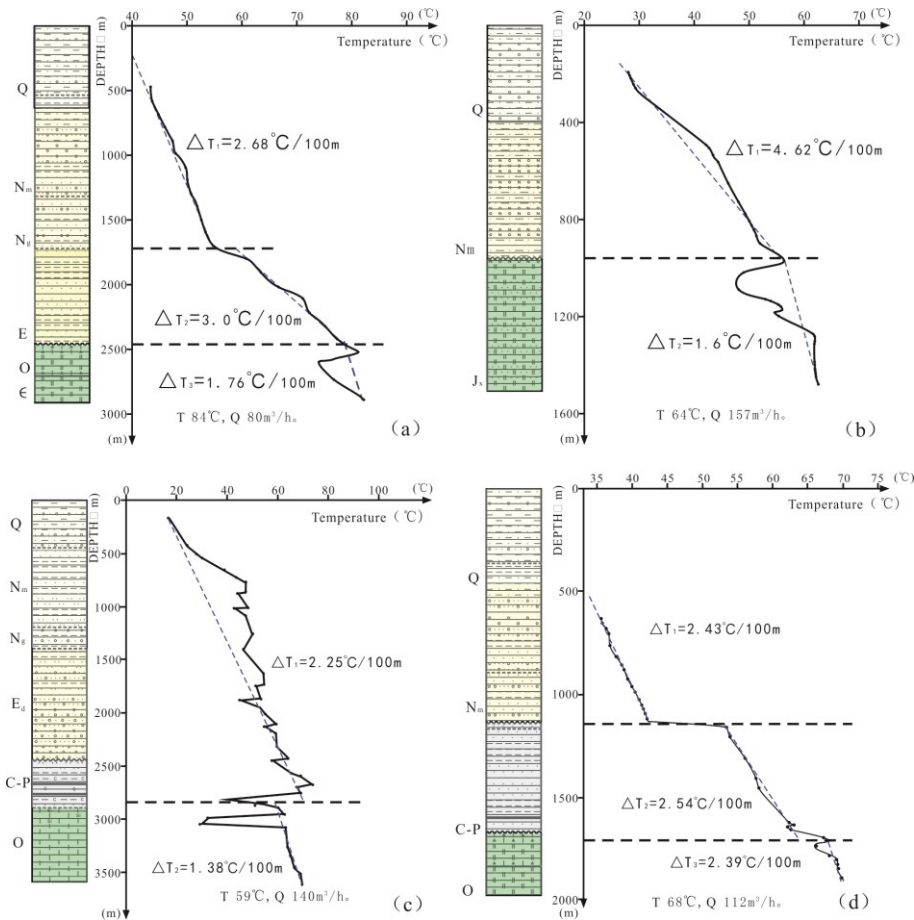


Figure 11: Typical drilling depth-temperature curves in Beijing-Tianjin-Hebei Plain.

a. Central International City 2 well in Xinji on Ningjin bulge, b. Hujiatai 1 well in Xiongxin on Niutuozen bulge, c. Lijingmingju 1 well in Gucheng on Wucheng bulge, d. Xinhe 12 well on Xinhe bulge.

The results are as follows:

(1) The geothermal gradient between the reservoir and the caprock in the bedrock bulge belt has obvious segmental refraction (Xiong et al., 1988), that is, the geothermal gradient of the geothermal reservoir is small, and the heat transfer rate is fast. The geothermal gradient of the caprock is large and the heat transfer rate is slow. It reflects the influence of the difference of thermal conductivity between carbonate geothermal reservoir and sand-shale caprock on heat transfer rate.

(2) In the southern part of the high bulge belt, the transfer velocity of geothermal heat in the geothermal reservoir is about 3 times than that of the caprock, and its thermal conductivity are 5.75 W/m·°C and 1.99 W/m·°C, respectively. In the Ningjin bulge and Wucheng bulge area, the transfer velocity of the geothermal heat in the geothermal reservoir is 1.7 times than that of the caprock, and its thermal conductivity is 4.26-5.80W/m·°C, 2.50-3.56 W/m·°C. This phenomenon indicates that the greater the amplitude of the bedrock bulge, the faster the heat transfer rate of the Karst heat reservoir in the bedrock, and the greater the difference from the thermal conductivity of the caprock.

(3) In the Xinhe bulge belt, the transfer rates of the geothermal heat in the reservoir and in the caprock are similar, which are  $2.72 \text{ W/m}\cdot\text{°C}$  and  $2.56 \text{ W/m}\cdot\text{°C}$ , respectively. It is speculated that the well is located near the fault zone, and the micro-fracture of the fault zone normalizes the reservoir and caprock, so that the heat transfer rate between them is basically the same.

**Table 2: Thermal conductivity of geothermal reservoir-caprock in the basement bulge belt of the Beijing-Tianjin-Hebei Plain.**

Exploration well	Location	Third grade structural units	Geothermal reservoir	Geothermal flow value ( $\text{mw/m}^2$ )	Geothermal gradient of geothermal reservoir ( $\text{°C}/100\text{m}$ )	Geothermal gradient of caprock ( $\text{°C}/100\text{m}$ )	Conductivity of geothermal reservoir ( $\text{w/m}\cdot\text{°C}$ )	Conductivity of caprock ( $\text{w/m}\cdot\text{°C}$ )
BZC 2well	Xiongxian	Niutuozhen bulge	Jxw	92	1.6	4.62	5.75	1.99
GJC2 well	Xinji	Ningjin bulge	O+E	75	1.76	3.0	4.26	2.50
LJMZ2 well	Gucheng	Wucheng bulge	O+E	80	1.38	2.25	5.80	3.56
XH10 well	Xinhe	Xinhe bulge	O	65	2.39	2.54	2.72	2.56

#### 4. GEOTHERMAL RESERVOIR CONCEPTUAL MODEL

Through the above research on the reservoir-caprock assemblage, geothermal water recharge source, migration channel and heat transfer pattern of Karst geothermal system, the conceptual model of Karst geothermal system in the Beijing-Tianjin-Hebei Plain is established. It is considered that: in the background of the high geothermal flow value of the large rift basin, the atmospheric precipitation in the west side of the Taihang Mountains and in the north of the Yanshan Karst bare area is the recharge water source, the deep marginal fault and the Karst unconformity as the migration channel. After cycling heating, the low-medium temperature conductive aquifer system formed by enrichment and pressure in Karst reservoirs in the bedrock bulge belt of the basin (Figure 12). The geothermal system has the following three characteristics: (1) The recharge source area of geothermal water is near, but the migration distance in the basin is long. Due to the large area of the faulted basin, the recharge water from Taihang Mountain and Yan Mountain is transported and drained to the sea by the basin's bedrock bulge area (basin low-pressure zone), that the distance is more than 400km and the time required for migration is about 25ka. (2) There are six types of reservoir and cap combinations. The different tectonic belts in the study area are affected by the difference of the degree of denudation between the Indosinian and Yanshanian periods. The two sets of Karst geothermal reservoirs that the Wumishan Formation of the Jixian System and the Ordovician Formation are mainly developed. Six types of reservoir-cap combinations have been developed. (3) The high-quality geothermal resources are mainly distributed along the basement bulge belt. The central bulge belt of the Jizhong depression and the Cangxian uplift belt are both favorable Karst facies belts, and relatively shallower buried belts of Karst geothermal reservoir, thus they are the high-quality geothermal resource distribution belts for Karst geothermal reservoir.

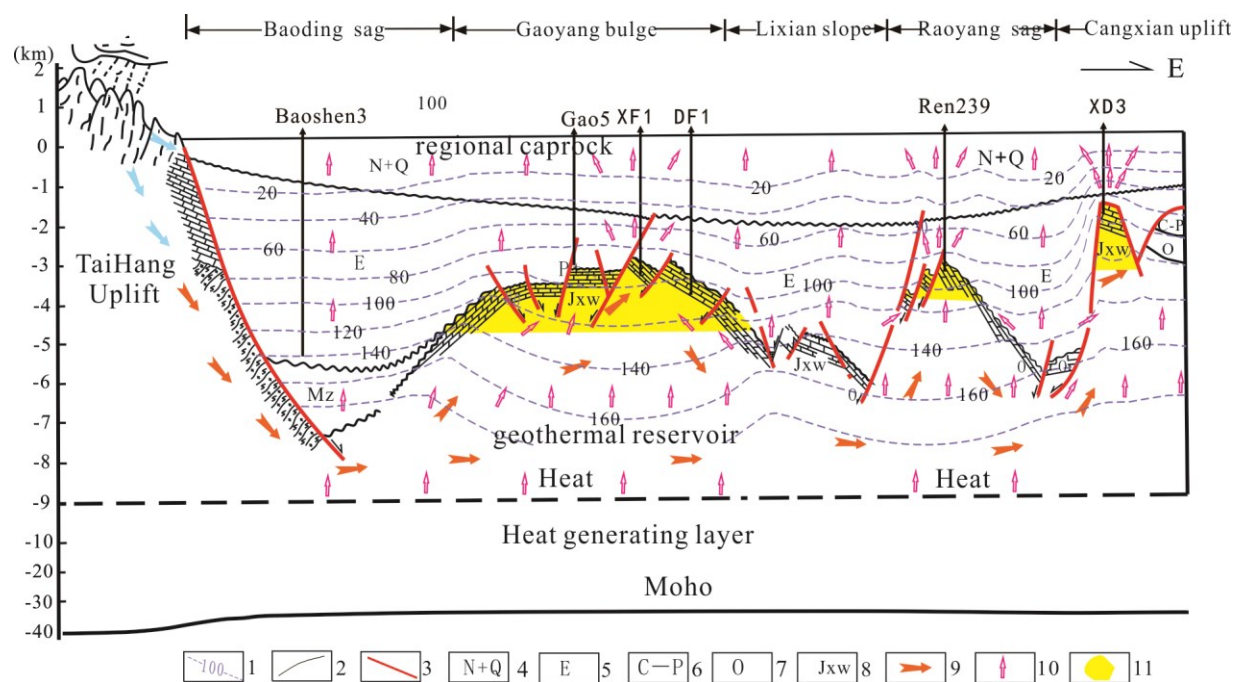


**Figure 12: The map of Karst geothermal system conceptual model in the Beijing-Tianjin-Hebei Plain.**

1. Temperature contour ( $\text{°C}$ ), 2. Stratigraphic boundary, 3. Fault, 4. Neogene - Quaternary, 5. Palaeogene., 6. Carboniferous - Permian, 7. Ordovician, 8. Wumishan formation, 9. Flow direction, 10. Heat direction, 11. Geothermal reservoir.

## 5. GEOTHERMAL RESOURCE EVALUATION

### 5.1 Calculation formula

The above conceptual model shows that the geothermal reservoir type of the Karst geothermal system in the Beijing-Tianjin-Hebei Plain is a conductive layered geothermal reservoir that developed in the sedimentary basin. Therefore, under the support of the aforementioned Karst geothermal reservoir thickness, porosity, roof temperature and other research results, the "thermal storage volume method" can be used to evaluate the geothermal resources of the Karst geothermal system. The "thermal storage volume method" calculation includes two parts: the heat storage of the rock in the geothermal reservoir and the heat carried by the geothermal water. The specific calculation formula is:

$$Q = Ad \left[ P_c C_c (1 - \phi) + \phi P_w C_w \right] (t_r - t_0) \quad (1)$$

Where,  $Q$ ,  $A$ ,  $d$ ,  $\phi$ ,  $t_r$ ,  $t_0$ ,  $P_c$ ,  $P_w$ ,  $C_c$ ,  $C_w$  are geothermal resources capacity (J), evaluation area (m<sup>2</sup>), geothermal reservoir effective thickness (m), rock porosity (dimensionless), geothermal reservoir temperature (°C), average annual temperature (°C), density of rock (kg/m<sup>3</sup>), density of water (kg/m<sup>3</sup>), specific heat capacity of rock (J/(kg·°C)), specific heat capacity of water (J/(kg·°C)).

### 5.2 Determination of physical parameters of geothermal reservoirs

The resource evaluation targets mainly have two sets of Karst heat reservoirs: the Wumishan Formation of the Jixian System and the Ordovician Formation. The calculation method is to use the geothermal resource evaluation software to perform grid processing by 1×1km by computer, and then divide the three blocks of Beijing, Tianjin and Hebei to calculate the weighted average as the main parameters to the calculation of the thermal storage method (table 3). The main parameters include:

(1) Area of study area (A): According to the distribution range of the remaining the Wumishan Formation of the Jixian System and Ordovician Formation Karst heat reservoirs, then superimposes the administrative boundaries of the regions of Beijing, Tianjin and Hebei in computer software, and calculates the layer's distribution area of each block. For example, the area of the Ordovician geothermal reservoir in Hebei, Beijing, and Tianjin are 66,791.807 km<sup>2</sup>, 5,292.26 km<sup>2</sup>, and 10,088.34 km<sup>2</sup>, respectively.

(2) Effective thickness (d) and porosity ( $\phi$ ) of geothermal reservoir: the effective thickness and porosity contour distribution of the geothermal reservoir is treated in a grid shape of 1×1km, and calculate the weighted average of each gridded data point, then obtain the average value of the effective thickness and porosity of each block. For example, the effective thickness of the Ordovician geothermal reservoir in Hebei, Beijing, and Tianjin are 110.26m, 116.76m, and 97.08m, respectively; the average porosity are 0.0331, 0.0319, and 0.0358, respectively.

(3) Geothermal reservoir temperature ( $t_r$ ): firstly, according to the above method, the isoline of the temperature distribution of the Karst geothermal reservoir roof is 1×1km gridded, and the weighted average temperature of the top surface of three blocks (Beijing, Tianjin and Hebei) is calculated. Secondly, the average geothermal reservoir temperature of each block is calculated: the geothermal reservoir temperature = roof temperature + geothermal gradient × formation thickness × 1/2 (the geothermal gradient of the Ordovician Formation and the Wumishan Formation of the Jixian System are 2.4 °C /100m and 2.1 °C /100m). For example, the average geothermal temperatures in Hebei, Beijing, and Tianjin are 64.63 °C, 55.13 °C, and 61.17 °C, respectively.

(4) Other parameters: the local average annual temperature is 12.5 °C, the geothermal water density is 1,000kg/m<sup>3</sup>, the rock density is 2881kg/m<sup>3</sup>, the water specific heat is 4180 J/(kg·°C); the rock specific heat is 940 J/(kg·°C).

### 5.3 Analysis of evaluation results

Table 3 shows the geothermal resources calculated by the zonal and stratified systems of the Karst geothermal system in the Beijing-Tianjin-Hebei Plain. According to statistics, the total amount of geothermal resources is 538.21×10<sup>8</sup>GJ, which is equivalent to 1,841.55×10<sup>8</sup>t of standard coal (1t standard coal can produce 29.3GJ heat). According to GB/T 11615-2010, the recovery rate of Karst geothermal reservoir is 15%, and the recoverable resource of Karst geothermal system in the Beijing-Tianjin-Hebei Plain is 80.74×10<sup>8</sup>GJ, equivalent to 276.23×10<sup>8</sup>t of standard coal. According to the maximum depth that can be achieved by existing geothermal drilling, some scholars refer to the geothermal resources in shallower than 4km in depth as the economic resources. In the Beijing-Tianjin-Hebei Plain, according to the above results, two sets of Karst geothermal reservoirs' resource in shallower than 4km in depth can be calculated by software as 431.98×10<sup>8</sup>GJ, which is equivalent to 1,478.05×10<sup>8</sup>t of standard coal. The recoverable geothermal resource is 64.80×10<sup>8</sup>GJ, which is equivalent to 221.71×10<sup>8</sup>t of standard coal. If it could be mined for 100 years, the amount of geothermal resources that can be mined per year is equivalent to 2.22 × 10<sup>8</sup>t of standard coal. According to the calculation of the heat required for heating per square meter per year which is equivalent to 0.029 t of standard coal, the heating area of the Beijing-Tianjin-Hebei Plain with only 4,000 meters of shallow economic geothermal resources can reach 76.45×10<sup>8</sup> square meters. In view of the fact that the geothermal heating area currently built is only 40 million square meters, the development prospect is broad.

**Table 3: Evaluation parameters and calculation results for geothermal resources of Karst geothermal system in the Beijing-Tianjin-Hebei Plain**

Reservoir	Location	Evaluation area (km <sup>2</sup> )	Average thickness (m)	Average temperature (°C)	Average porosity (%)	Geothermal resources (10 <sup>16</sup> KJ)	Standard coal (10 <sup>8</sup> t)	Recoverable resources (10 <sup>16</sup> KJ)	Standard coal (10 <sup>8</sup> t)
O	Hebei	66,791.81	110.26	64.63	3.31	106.84	365.56	16.03	54.83
	Beijing	5,290.26	116.76	55.13	3.19	7.34	25.12	1.10	3.77
	Tianjin	10,088.34	97.08	61.17	3.58	13.29	45.49	1.99	6.82
Jxw	Hebei	57,880.23	266.77	80.37	4.53	292.92	1002.25	43.94	150.34
	Beijing	5,290.28	398.98	77.53	3.83	38.24	130.86	5.74	19.63
	Tianjin	10,611.97	390.21	81.35	4.28	79.58	272.27	11.94	40.84
Total						538.21	1841.55	80.74	276.23

## 6. CONCLUSIONS

(1) The generation and evolution of the Karst geothermal system in the Beijing-Tianjin-Hebei Plain mainly underwent five stages: the Mesoproterozoic-Early Paleozoic platform-type marine carbonate deposition stage, the Late Paleozoic direct caprock development stage, the Mesozoic uplift and denudation and buried hill Karst development stage, the Paleogene extensional fault block differential uplift and fall and fault-related Karst development stage, the Neogene regional geothermal reservoir caprock deposition and the formation of geothermal water-bearing system.

(2) The Karst geothermal system of the Beijing-Tianjin-Hebei Plain is mainly composed of Jixian Wumishan and Ordovician Formations, with six types of reservoir-caprock assemblage patterns identified. High-quality geothermal resources are mainly concentrated in two relatively shallow buried structural belts, the central uplift belt of Jizhong Depression and the Cangxian uplift belt. They are characterized by multiple Karstification stages (Caledonian, Indosinian, Yanshanian and Himalayan), large accumulated effective thickness (500-700m in Jixian Wumishan Formation, 100-140m in Ordovician System), good porosity (4-6%) and high thermal storage temperature (60-100 °C of roof temperature).

(3) Water migration within the Karst geothermal system is characterized as follows: the atmospheric precipitation from Taihang and Yanshan mountains enters the deep part of the basin through deep faults on the basin margin and the Karst unconformities, migrates along four main groundwater runoff directions (i.e. the low pressure zones of the basin such as the basement uplift zone and the tectonic transformation zone), and discharges eastward into Bohai Bay after confluence. The salinity of geothermal water varies from fresh water to low mineralized water to high mineralized water to brine along its migration path. The hydrochemical types also have the characteristics of evolution from simple to complex and then to simple. The retention time of Karst geothermal water in the basin is about 10-25 ka.

(4) The heat source of the Karst geothermal system in the Beijing-Tianjin-Hebei Plain comes from the high geothermal flow of the rift basin, and the heat transfer mode is mainly heat conduction. The geothermal field has the characteristics of differential accumulation of high heat flow value (64-92 mW/m<sup>2</sup>) in the bedrock uplift zone and low heat flow value (50-58 mW/m<sup>2</sup>) in the bedrock depression zone. Longitudinal geothermal field also has a stratified structure with smaller geothermal gradient (fast heat transfer rate) of geothermal reservoir and larger geothermal gradient (slow heat transfer rate) of caprock. The larger extent of bedrock uplift, the faster heat transfers in Karst geothermal reservoirs, and the difference between them is 2-3 times.

(5) The total amount of geothermal resources in the Karst geothermal system in the Beijing-Tianjin-Hebei Plain is 53.821 billion GJ, which is equivalent to 184.155 tons of standard coal. The annual recoverable geothermal resources of shallow Karst geothermal reservoirs within 4km of depth is equivalent to 222 million tons of standard coal and that can provide 7.65 billion square meters of heating space, which shows a great potential for geothermal development.

## REFERENCES

- Arnorsson, S.: Geothermal systems in Iceland: Structure and conceptual models - I. High-temperature area, *Geothermics*, 24, (1995), 603-629.
- Chang, J, Qiu, N.S., Zhao, X.Z., Xu, W., Xu, Q.C., Jin, F.M.: Present-day geothermal regime of the Jizhong depression in Bohai Bay basin, East China, *Chinese J Geophys*, 59, (2016), 1003-1016.
- Chen, Z.Y., Zhang, G.H., Xu, J.M.: Paleoclimate Record Deduced from Groundwater and Climate Change Implications of Groundwater Resources in North China, *Acta geoscientia sinica (Bulletin of the Chinese Academy of Geological Sciences)*, 19, (1998), 338-345.
- Dong, D.W., Li, L., Liu, J., Li, J.Y.: Cenozoic tectonic evolution in the north-central Jizhong Depression, *Oil & Gas Geology*, 34, (2013), 771-780.
- Gong, Y.L., Wang, L.S., Liu, S.W., Li, C., Han, Y.B., Li, H.: Distribution characteristics of terrestrial heat flow in Jiyang Depression, *Science in China(D)*, 33, (2003), 384-391.

WANG et al.

- He, Z.L., Feng, J.Y., Zhang, Y., Li, P.W.: A tentative discussion on an evaluation system of geothermal unit ranking and classification in China, *Earth Science Frontiers*, 24, (2017), 168-179.
- Helgeson, H.C.: Geologic and thermodynamic characteristics of Salton Sea geothermal system, *American Journal of Science*, 266, (1968), 129-166.
- Mao, X.P.: Genetic Mechanism and Distribution Characteristics of High Temperature Anomaly in Geothermal Field, *Acta Geoscientica Sinica*, 39, (2018), 216-224.
- Moeck, I.S.: Catalog of geothermal play types based on geologic controls. *Renewable & Sustainable Energy Reviews*, 37, (2014), 867-882.
- Muffler, L.J.P., Williams, D.L.: Geothermal investigations of the U. S. Geological Survey in Long Valley, California, 1972—1973, *Journal of Geophysical Research*, 81, (1976), 721-724.
- Nukman, M., Moeck, I.: Structural controls on a geothermal system in the Tarutung Basin, north central Sumatra, *Journal of Asian Earth Sciences*, 74, (2013), 86-96.
- Qiao, H.S., Fang, C.L., Niu, J.Y., Guan, D.S.: Petroleum geology of deep horizon in Bohaiwan Basin. Beijing: *Petroleum Industry Press*, (2002).
- Rybach, L.: Classification of geothermal resources by potential, *Geothermal Energy Science*, 3, (2015), 13-17.
- Wang, L.S., Liu, S.W., Xiao, W.Y., Li, C., Li, H., Guo, S.P.: Distribution characteristics of terrestrial heat flow in Bohai Bay Basin, *Chinese science bulletin*, 47, (2002), 151-155.
- Wu, K.Y., Wang, Y.J.: Palaeo-Karst development model of the Pre-Tertiary carbonate rock in Jizhong depression, *Carsologica Sinica*, 29, (2010), 56-63.
- Xiong, L.P., Zhang, J.M.: Relationship between geothermal gradient and the relief of basement rock in North China plain, *Acta Geophysica Sinica*, 31, (1988): 146-155.
- Yan, D.S., Yu, Y.T.: Evaluation and utilization of geothermal resources in oil and gas area of Beijing-Tianjin-Hebei. Wuhan: *China University of Geosciences Press*, (2000).
- Yang, M.H.: Transfer structure and its relation to hydrocarbon exploration in Bohai Bay Basin, *Acta Petrolei Sinica*, 30, (2009), 816-823.
- Zhang, G.H., Chen, Z.Y., Fei, Y.H.: Relationship between the Formation of Groundwater and the Evolution of Regional Hydrologic Cycle in North China Plain, *Advances In Water Science*, 11, (2000), 415-420.
- Zhang, W.C., Cui, Z.Q., Han, C.Y., Guo, Y.J., Wang, H.S., Li, L.: Evolution of palaeogene lacustrine basins and oil and gas potentials in the central Hebei depression, *Journal of Palaeogeography*, 3, (2001), 45-54.
- Zhang, Y., Feng, J.Y., He, Z.L., Li, P.W.: Classification of geothermal systems and their formation key factors, *Earth Science Frontiers* 24, (2001), 190-198.
- Zhou, R.L.: The activity of deep underground water in the northern part of the North China Plain and its effect on the Geothermal field. *China Academy of Geological Sciences of 562 Brigade*, 6, (1987), 17-35.